

Title	High-quality surface passivation of crystalline silicon with chemical resistance and optical transparency by using catalytic chemical vapor deposition SiN <sub>x</sub> layers and an ultrathin SiO <sub>x</sub> film
Author(s)	Tu, Huynh Thi Cam; Koyama, Koichi; Nguyen, Cong Thanh; Ohdaira, Keisuke; Matsumura, Hideki
Citation	Japanese Journal of Applied Physics, 57(8S3): 08RB17-1-08RB17-4
Issue Date	2018-07-17
Type	Journal Article
Text version	author
URL	<a href="http://hdl.handle.net/10119/16764">http://hdl.handle.net/10119/16764</a>
Rights	This is the author's version of the work. It is posted here by permission of The Japan Society of Applied Physics. Copyright (C) 2018 The Japan Society of Applied Physics. Huynh Thi Cam Tu, Koichi Koyama, Cong Thanh Nguyen, Keisuke Ohdaira, and Hideki Matsumura, Japanese Journal of Applied Physics, 57(8S3), 2018, 08RB17. <a href="https://doi.org/10.7567/JJAP.57.08RB17">https://doi.org/10.7567/JJAP.57.08RB17</a>
Description	

# **High-quality surface passivation of crystalline silicon with chemical resistance and optical transparency by using catalytic chemical vapor deposition SiN<sub>x</sub> layers and an ultrathin SiO<sub>x</sub> film**

Huynh Thi Cam Tu<sup>1</sup>, Koichi Koyama<sup>2</sup>, Cong Thanh Nguyen<sup>1</sup>, Keisuke Ohdaira<sup>1</sup>, and Hideki Matsumura<sup>1</sup>

<sup>1</sup> *Japan Advanced Institute of Science and Technology, Nomi, Ishikawa 923-1292, Japan*

<sup>2</sup> *ULVAC, Inc., Chigasaki, Kanagawa 253-8543, Japan*

We have developed high-quality surface passivation films for n-type crystalline silicon (c-Si) with an effective minority carrier lifetime ( $\tau_{\text{eff}}$ ) of more than 6 ms or a maximum surface recombination velocity ( $\text{SRV}_{\text{max}}$ ) of less than 2 cm/s using two highly optically transparent silicon nitride (SiN<sub>x</sub>) layers and an ultrathin SiO<sub>x</sub> film. First, an ultrathin SiO<sub>x</sub> film is unintentionally formed on the surface of c-Si by annealing c-Si in N<sub>2</sub> ambient at 350 °C. Then, on the SiO<sub>x</sub> film, two SiN<sub>x</sub> layers are sequentially formed at substrate temperatures ( $T_{\text{sub}}$ ) of 100 and 250 °C by catalytic chemical vapor deposition (Cat-CVD), often called hot-wire CVD. With the combination of the ultrathin SiO<sub>x</sub> film and the two SiN<sub>x</sub> layers, we can obtain a novel passivation structure with high-quality surface passivation, high optical transparency, and high chemical resistance for subsequent processes.

## 1. Introduction

Reduction of total fabrication cost and enhancement of the conversion efficiency of solar cells are the major requirements in research in the photovoltaic (PV) community. For crystalline silicon (c-Si)-based solar cells, which occupy the largest share of the PV market (> 90%), these requirements become more severe. The basis for achieving high-efficiency solar cells is decreasing the total amount of loss, i.e., optical and electrical losses <sup>1)</sup>. Over many years of effort in solving these issues, the efficiency of c-Si solar cells has been significantly improved. Indeed, so far, the efficiency of c-Si solar cells prepared using heterojunction (HJ) and interdigitated back contact (IBC) structures has reached up to 26.37% <sup>2)</sup> and 26.7% <sup>3)</sup>. However, it should be noted that the front surface of this solar cell is passivated with an amorphous silicon (a-Si) layer through which short-wavelength sunlight can be easily absorbed <sup>4-8)</sup>. This type of optical loss may limit further improvement of the efficiency of c-Si solar cells. Therefore, it is required to develop a high-quality passivation layer with high optical transparency. In addition, the front passivation layer should be chemically resistive, which will be mentioned below.

In our research group, we have succeeded in fabricating very high-quality passivation layers using silicon nitride (SiN<sub>x</sub>)/intrinsic-a-Si (i-a-Si) stacked layers formed by catalytic chemical vapor deposition (Cat-CVD), often called hot-wire CVD <sup>9)</sup>. The maximum surface recombination velocity ( $SRV_{\max}$ ), which is evaluated under the assumption that no carrier recombination occurs inside the bulk c-Si, is lower than 1.5 cm/s for such passivation <sup>10-12)</sup>. Furthermore, instead of using the a-Si layer, we have developed a new passivation structure in which a Cat-CVD SiN<sub>x</sub> film is deposited at a substrate temperature ( $T_{\text{sub}}$ ) of 100 °C on a phosphorous (P) Cat-doped c-Si <sup>13)</sup>. With this structure, we were able to obtain a  $SRV_{\max}$  of as low as 2 cm/s. However, we realized that SiN<sub>x</sub> deposited at such a low  $T_{\text{sub}}$  has a rather high

etch rate in hydrofluoric acid (HF). In the processing of the rear side of an IBC solar cell, the passivation layer may be damaged by various treatments in some chemical solutions such as HF and alkaline solution<sup>14, 15)</sup>. If the passivation layer is easily etched by these solutions, its passivation quality becomes worse, which degrades cell efficiency. Therefore, to obtain a high-efficiency solar cell, a passivation layer with high chemical resistivity is strongly required. Otherwise, we should cover the solar cell with a protective film<sup>16)</sup>.

In contrast to a  $\text{SiN}_x$  film deposited at a low  $T_{\text{sub}}$ , that prepared at high temperatures ( $> 200$  °C) exhibits a low etch rate in HF solution. In particular, it is known that  $\text{SiN}_x$  films formed by Cat-CVD at a high  $T_{\text{sub}}$  are more chemically resistive than those prepared by conventional plasma-enhanced chemical vapor deposition (PECVD)<sup>17-22)</sup>. For example, in a buffered HF (BHF) solution, the etch rate of Cat-CVD  $\text{SiN}_x$  is about 1/5 lower than that of PECVD  $\text{SiN}_x$ <sup>21, 22)</sup>. Therefore, to take advantage of this feature, we decided to fabricate a two-layered structure of a high- $T_{\text{sub}}$   $\text{SiN}_x$  film (250 °C) on a low- $T_{\text{sub}}$   $\text{SiN}_x$  (100 °C) film to passivate the front surface of an IBC c-Si solar cell. However, the c-Si passivated by the two  $\text{SiN}_x$  layers has an effective minority carrier lifetime ( $\tau_{\text{eff}}$ ) of only about 3 ms or a  $SRV_{\text{max}}$  of 4.5 cm/s. Therefore, we made efforts to improve  $\tau_{\text{eff}}$  and discovered that  $\tau_{\text{eff}}$  can be increased to 6 ms by annealing c-Si substrates at 350 °C.

In this paper, we report a novel passivation structure for passivating well the front surface of IBC c-Si solar cells. The structure includes the two highly transparent  $\text{SiN}_x$  layers formed by Cat-CVD and the ultrathin  $\text{SiO}_x$  film formed by low-temperature annealing of c-Si. In addition, we demonstrate that the  $\text{SiN}_x$  layers have a rather low etching rate in a solution containing 5 to 9% HF, which facilitates the solar cell fabrication become by eliminating the need for any protective film.

## 2. Experimental procedure

270- $\mu\text{m}$ -thick double-sided mirror-polished n-type c-Si(100) wafers with resistivities of 1–5  $\Omega\text{ cm}$  were used in this study. The wafers were submerged in 5% HF solution for 30 s to remove the native oxide layers prior to annealing in a conventional quartz-tube furnace at a temperature of 350  $^{\circ}\text{C}$  for 30 min in various ambient gases, such as pure nitrogen ( $\text{N}_2$ ) and oxygen ( $\text{O}_2$ ). After annealing, the wafers were taken out of the furnace and cooled to room temperature in air atmosphere. Then, double  $\text{SiN}_x$  layers were sequentially deposited on the front and rear surfaces of the c-Si wafer by Cat-CVD. The first  $\text{SiN}_x$  layer was formed at  $T_{\text{sub}} < 150$   $^{\circ}\text{C}$ , while the second layer was fabricated at a higher  $T_{\text{sub}}$  of 250  $^{\circ}\text{C}$ . The thickness, refractive index ( $n$ ), and extinction coefficient ( $k$ ) of the  $\text{SiO}_x$  and  $\text{SiN}_x$  films were determined by spectroscopic ellipsometry. The parameters for Cat-CVD  $\text{SiN}_x$  film deposition as well as the thickness ( $t$ ),  $n$ , and  $k$  at a wavelength of 630 nm are summarized in Table I. Finally, the wafers were annealed on a hot plate at 350  $^{\circ}\text{C}$  for 30 min in air ambient, that is, post-deposition annealing. The  $\tau_{\text{eff}}$  of the Si wafers was analyzed at room temperature by microwave photoconductivity decay ( $\mu\text{-PCD}$ ; Kobelco LTA-1510EP) using a 904-nm-wavelength laser pulse with a photon density of  $5 \times 10^{13}\text{ cm}^{-2}$ . This generates photocarriers at densities of  $(2\text{--}3) \times 10^{15}\text{ cm}^{-3}$ , considering the optical absorption for light of 904 nm wavelength in 270- $\mu\text{m}$ -thick c-Si. All the processes for the fabrication of the samples described above are illustrated in Fig. 1.

## 3. Results and discussion

As mentioned above, when the  $\text{SiN}_x$  double layers were directly formed on the bare surfaces of the c-Si substrate,  $\tau_{\text{eff}}$  only reached up to about 3 ms. However, when the c-Si substrates were annealed at 350  $^{\circ}\text{C}$  prior to the first  $\text{SiN}_x$  deposition,  $\tau_{\text{eff}}$  increased significantly. Figure

2 shows  $\tau_{\text{eff}}$  when the c-Si substrates were annealed under various ambients. The  $T_{\text{sub}}$  values for depositing the first and second SiN<sub>x</sub> layers were 100 and 250 °C, respectively. As can be seen,  $\tau_{\text{eff}}$  of c-Si annealed in vacuum is almost the same as that without annealing. On the other hand,  $\tau_{\text{eff}}$  of c-Si annealing in O<sub>2</sub> or N<sub>2</sub> ambient was apparently improved. Thus, to determine the reason for this improvement, we observed the surfaces of these c-Si substrates by X-ray photoelectron spectroscopy (XPS). Figure 3 shows XPS data from the Si 2p emission region of the c-Si wafers annealed under vacuum, N<sub>2</sub>, and O<sub>2</sub> ambient conditions at 350 °C for 30 min. It is clearly seen that shoulder peaks appear near 103 eV assigned to Si-O bonding in the film, and the intensities of the peaks are likely dependent on the annealing ambient. That is, when c-Si substrates are annealed in the furnace in N<sub>2</sub> ambient, their surfaces are oxidized. As mentioned above, after annealing at 350 °C the wafers were cooled to room temperature in air ambient. We confirmed that a SiO<sub>x</sub> layer is formed during this cooling process. In addition, when the wafers were annealed at 350 °C in air ambient, the results are almost the same as those obtained by annealing in O<sub>2</sub> ambient. Table II shows the thickness and  $n$ , determined by spectroscopic ellipsometry at a wavelength of 630 nm, of the SiO<sub>x</sub> layers formed by annealing under N<sub>2</sub> and O<sub>2</sub> ambient conditions. The refractive indices of both samples are about 1.3 to 1.35, near that of stoichiometric SiO<sub>2</sub> ( $n = 1.45$ ). Moreover, the thickness of the present SiO<sub>x</sub> is in the range from 0.8 to 1.0 nm for annealing in N<sub>2</sub> ambient and about 1.3 nm for annealing in pure O<sub>2</sub> ambient. Therefore, Fig. 2 shows that the SiO<sub>x</sub> layer with a thickness less than 1 nm, which is formed in N<sub>2</sub> ambient, exhibits a slightly better passivation quality when SiN<sub>x</sub> layers are formed on it.

In order to determine the actual effect of the existence of SiO<sub>x</sub> in improving the c-Si surface passivation quality, we performed capacitance-voltage (C-V) measurement of two MOS structures: Al/ SiN<sub>x</sub> double layers/SiO<sub>x</sub>/n-c-Si/Al and Al/ SiN<sub>x</sub> double layers/n-c-Si/Al.

The double SiN<sub>x</sub> layers were deposited at the  $T_{\text{sub}}$  of 100 and 250 °C, and the SiO<sub>x</sub> layer was formed by thermal annealing at 350 °C for 30 min in N<sub>2</sub> ambient. Post-deposition annealing at 400 °C for 10 min was conducted to form an ohmic contact between Al and c-Si. The results are shown in Fig. 4. It is clearly seen that the C-V curve is strongly shifted towards negative voltages by SiO<sub>x</sub> insertion between the n-c-Si and the double SiN<sub>x</sub> layers. This shift indicates the existence of a large number of net positive fixed charges at the interface between the c-Si and the double SiN<sub>x</sub> layers. The formation of the thin SiO<sub>x</sub> film is considered to generate positively charged, donor-like states at the surface of c-Si, which results in a downward bending of the bands near its surface. Simplified energy band diagrams of n-type c-Si with and without the thin SiO<sub>x</sub> film are shown in Fig. 5. Downward band bending gives rise to an electric field, which tends to repel minority carriers (i.e., holes) from the surface of c-Si. Therefore, the recombination rate of holes and electrons near the surface of c-Si decreases or the lifetime of minority carriers increases. Since the gradients of the C-V curves of both samples do not appear markedly different, the interface state density may not be markedly changed, compared with the difference in the density of fixed charges. We confirmed that the introduction of the ultrathin SiO<sub>x</sub> film changes the surface potential of c-Si, which leads to the improvement of  $\tau_{\text{eff}}$ .

We have reported that when SiN<sub>x</sub> is deposited directly on c-Si at  $T_{\text{sub}}$  from 250 to 350 °C, N atoms are likely to penetrate into c-Si, which may cause the generation of new defects in c-Si<sup>23)</sup>. However, when we insert a thin i-a-Si layer between SiN<sub>x</sub> and c-Si, the N penetration can be prevented and  $\tau_{\text{eff}}$  can be improved markedly<sup>24)</sup>. Actually, from the results of scanning transmission electron microscopy (STEM) and energy dispersive X-ray spectroscopy (EDS) measurements, N penetration appears to be suppressed in the sample with a high  $\tau_{\text{eff}}$ <sup>23)</sup>. Furthermore, it is assumed that N penetration may be more suppressed if the

$T_{\text{sub}}$  of the first  $\text{SiN}_x$  is low enough. Figure 6 shows the dependence of  $\tau_{\text{eff}}$  on  $T_{\text{sub}}$  for depositing the first  $\text{SiN}_x$  layer. This figure appears to show that a lower  $T_{\text{sub}}$  for the first  $\text{SiN}_x$  layer is suitable for attaining a better  $\tau_{\text{eff}}$ .

Moreover, the lower  $T_{\text{sub}}$  for depositing the  $\text{SiN}_x$  layer may induce another effect. It is reported that the  $\text{SiN}_x$  film deposited at a low  $T_{\text{sub}}$  is a source of hydrogen (H). By annealing, these H atoms can diffuse into the c-Si and terminate the defects at its surface<sup>25</sup>), thereby enhancing the quality of the c-Si<sup>26-30</sup>). Figure 7 shows the concentration of H atoms in the  $\text{SiN}_x$  films as a function of  $T_{\text{sub}}$ . The H concentration was calculated using Eq. (1) on the basis of the FT-IR spectra shown in the inset of Fig. 7. For details of the calculation method, we refer to Ref. 31.

$$N_H = \left( \frac{A_{\text{Si-H}}}{0.57 \times 10^{-19}} + \frac{A_{\text{N-H}}}{0.48 \times 10^{-19}} \right) \frac{1}{d} \quad (1)$$

Where,  $N_H$ ,  $d$ ,  $A_{\text{Si-H}}$ , and  $A_{\text{N-H}}$  are the H concentration, the thickness of the absorbance layer, and the height of Si-H and N-H absorbance peaks, respectively.

It is clearly seen from Fig. 6 that the H concentration in the  $\text{SiN}_x$  film likely decreases when the  $T_{\text{sub}}$  of the  $\text{SiN}_x$  layer increases. Therefore, the slight drop in  $\tau_{\text{eff}}$  with the increase in  $T_{\text{sub}}$  of the first  $\text{SiN}_x$  layer shown in Fig. 5 can be explained as being due to the reduction in H content, thereby decreasing the number of defects terminated by H, which results in the degradation of passivation quality. In order to realize good passivation quality, the first  $\text{SiN}_x$  layer should be fabricated at a low  $T_{\text{sub}}$ .

Finally, we show the chemical resistivity of the present system. Figure 8 shows the etch rates of Cat-CVD  $\text{SiN}_x$  films in 5 and 9% HF solutions as a function of  $T_{\text{sub}}$ . In addition, the etch rates of PECVD  $\text{SiN}_x$  in the buffered HF (BHF) solution containing 7–9% HF diluted in an aqueous solution of 40% ammonium fluoride ( $\text{NH}_4\text{F}$ ) are also shown for reference<sup>18-20</sup>).



The etch rates of the SiN<sub>x</sub> films deposited at  $T_{\text{sub}}$  above 250 °C are rather low, about 2.5 to 5 nm/min in 5% HF solution or from 7 to 9.5 nm/min in 9% HF solution. This means that the SiN<sub>x</sub> double-layer structure with the second layer prepared at  $T_{\text{sub}} = 250$  °C has high chemical resistivity, which appears applicable to the fabrication of high-efficiency solar cells without the need for any protective film. The etch rates of PECVD SiN<sub>x</sub> formed at  $T_{\text{sub}} = 300$  °C or more are from 10 to 60 nm/min, which are higher than those of Cat-CVD SiN<sub>x</sub> formed at  $T_{\text{sub}} = 150$  °C. These results demonstrate the advantage of using Cat-CVD films in our present systems.

#### **4. Conclusions**

We have developed a novel and facile structure of double SiN<sub>x</sub> layers prepared by Cat-CVD and an ultrathin SiO<sub>x</sub> film formed at a low temperature for passivating the surfaces of n-type c-Si. The c-Si passivated by this structure exhibits high-quality surface passivation, good chemical resistivity, and high optical transparency, which are promising for obtaining high-efficiency IBC solar cells and reducing total fabrication cost.

#### **Acknowledgement**

This work was financially supported by a NEDO project, Japan.

## Reference

- 1) A. Goetzberger, J. Knobloch, and B. Voss, *Crystalline Silicon Solar Cells* (Wiley, New York, 1998) p. 89.
- 2) K. Yoshikawa, H. Kawasaki, W. Yoshida, T. Irie, K. Konishi, K. Kanako, T. Uto, D. Adachi, M. Kanemastu, H. Uzu, and K. Yamamoto, *Nat. Energy* **2**, 17032 (2017).
- 3) M. A. Green, Y. Hishikawa, W. Warta, A. D. Dunlop, D. H. Levi, J. H. Ebinger, and A. W. Y. H. Baillie, *Prog. Photovoltaics* **25**, 668 (2017).
- 4) M. Taguchi, A. Yano, S. Tohoda, K. Matsuyama, Y. Nakamura, T. Nishiwaki, K. Fujita, and E. Maruyama, *IEEE J. Photovoltaics* **4**, 96 (2014).
- 5) T. C. Thi, K. Koyama, K. Ohdaira, and H. Matsumura, *Sol. Energy Mater. Sol. Cells* **100**, 169 (2012).
- 6) M. Tanaka, M. Taguchi, T. Matsuyama, T. Sawada, S. Tsuda, S. Nakano, H. Hanafusa, and Y. Kuwano, *Jpn. J. Appl. Phys.* **31**, 3518 (1992).
- 7) H. Fujiwara and M. Kondo, *J. Appl. Phys.* **101**, 054516 (2007).
- 8) N. Jensen, R. M. Hausner, R. B. Bergmann, J. H. Werner, and U. Rau, *Prog. Photovoltaics* **10**, 1 (2002).
- 9) H. Matsumura, *J. Appl. Phys.* **65**, 4396 (1989).
- 10) K. Koyama, K. Ohdaira, and H. Matsumura, *Appl. Phys. Lett.* **97**, 082108 (2010).
- 11) K. Koyama, K. Ohdaira, and H. Matsumura, *Thin Solid Films* **519**, 4473 (2011)
- 12) C. T. Nguyen, K. Koyama, S. Terashima, C. Okamoto, S. Sugiyama, K. Ohdaira, and H. Matsumura, *Jpn. J. Appl. Phys.* **56**, 056502 (2017).
- 13) T. C. Thi, K. Koyama, K. Ohdaira, and H. Matsumura, *J. Appl. Phys.* **116**, 044510 (2014).
- 14) M. Lu, U. Das, A. Bowden, S. Hegedus, and R. Birkmire, *Prog. Photovoltaics* **19**, 326 (2011).
- 15) E. Franklin, K. Fong, K. McIntosh, A. Fell, A. Blakers, T. Kho, D. Walter, D. Wang, N. Zin, M. Stocks, E. Wang, N. Grant, Y. Wan, Y. Yang, X. Zhang, Z. Feng, and P. J. Verlinden *Prog. Photovoltaics* **24**, 411 (2014).
- 16) J. Nakamura, N. Asano, T. Hieda, C. Okamoto, H. Katayama, and K. Nakamura, *IEEE J. Photovoltaics* **4**, 1491 (2014).
- 17) T. C. T. Huynh, S. Terashima, K. Koyama, C. T. Nguyen, and H. Matsumura, *Proc. 32<sup>nd</sup> European Photovoltaic Solar Energy Conf.*, 2016, p. 606.
- 18) K. R. Williams, K. Gupta, and M. Wasilik, *J. Microelectromech. Syst.* **12**, 761 (2003).
- 19) V. Gottschalch, R. Schmidt, B. Rheinlander, D. Pudis, S. Hardt, J. Kvietkova, G. Wagner, and R. Franzheld, *Thin Solid Films* **416**, 224 (2002).

- 20) C. W. Pearce, R. F. Fetcho, M. D Gross, R. F. Koefer, and R. A. Pudliner, *J. Appl. Phys.* **71**, 1838 (1992).
- 21) Y. Uchiyama, A. Masuda, and H. Matsumura, *Thin Solid Films* **395**, 275 (2001).
- 22) H. Matsumura, *Thin Solid Films* **395**, 1 (2001).
- 23) K. Higashimine, K. Koyama, K. Ohdaira, H. Matsumura, and N. Otsuka, *J. Vac. Sci. Technol. B*, **30**, 031208 (2012).
- 24) K. Koyama, T. C. Thi, K. Higashimine, K. Ohdaira, and H. Matsumura, *Proc. 40<sup>th</sup> IEEE Photovoltaic Specialists Conf.*, 2014, p. 3304.
- 25) T. C. Thi, K. Koyama, K. Ohdaira, and H. Matsumura, *Jpn. J. Appl. Phys.* **55**, 02BF09 (2016).
- 26) T. C. Thi, K. Koyama, K. Ohdaira, and H. Matsumura, *Jpn. J. Appl. Phys.* **53**, 022301 (2014).
- 27) T. C. Thi, K. Koyama, K. Ohdaira, and H. Matsumura, *Thin Solid Films* **575**, 60 (2015).
- 28) D. K. Biegelsen, R. A. Street, C.C. Tsai, and J. C. Knights, *Phys. Rev. B* **20**, 4839 (1979).
- 29) Y. Larionova, V. Mertens, N. P. Harder, and R. Brendel, *Appl. Phys. Lett.* **96**, 032105 (2010).
- 30) H. Meddeb, T. Bearda, Y. Abdelraheem, H. Ezzaouia, I. Gordon, J. Szlufcik, and J. Poortmans, *J. Phys. D* **48**, 415301 (2015).
- 31) W. A. Lanford and M. J. Rand, *J. Appl. Phys.* **49**, 2473 (1978).

## Figure captions:

Fig. 1. (Color online) Process flow for preparing samples for measuring  $\tau_{eff}$ .

Fig. 2. (Color online)  $\tau_{eff}$  under various initial annealing conditions of c-Si substrates.

Fig. 3. (Color online) XPS data from Si 2p emission region of the c-Si substrate annealed under various ambient conditions

Fig. 4. (Color online) C-V curves of Al/SiN<sub>x</sub> double layers/SiO<sub>x</sub>/n-c-Si/Al (*with SiO<sub>x</sub>*) and Al/SiN<sub>x</sub> double layers/n-c-Si/Al (*without SiO<sub>x</sub>*).

Fig. 5. (Color online) Energy band diagrams of n-type c-Si with and without SiO<sub>x</sub>

Fig. 6. (Color online) Dependence of  $\tau_{eff}$  of c-Si passivated with SiN<sub>x</sub> double layers on  $T_{sub}$  for depositing the first SiN<sub>x</sub> layer. The 1-nm-thick-SiO<sub>x</sub> film beneath the SiN<sub>x</sub> double layers was grown in N<sub>2</sub> ambient at 350 °C.

Fig. 7. (Color online) Hydrogen concentration in SiN<sub>x</sub> deposited from 50 to 150 °C.

Fig. 8. (Color online) Etch rates of Cat-CVD SiN<sub>x</sub> in 5 and 9% HF solutions and of PECVD SiN<sub>x</sub> in BHF solutions containing 7-9% HF as a function of  $T_{sub}$ .

Table I. Parameters for Cat-CVD SiN<sub>x</sub> film deposition as well as thickness, *n*, and *k* determined by spectroscopic ellipsometry at wavelength of 630 nm.

	<i>FR</i> <sup>a</sup> (sccm)	<i>T</i> <sub>cat</sub> <sup>b</sup> (°C)	<i>P</i> <sub>g</sub> <sup>c</sup> (Pa)	<i>T</i> <sub>sub</sub> (°C)	Time (s)	<i>t</i> (nm)	<i>n</i>	<i>k</i>
First SiN <sub>x</sub> layer	SiH <sub>4</sub> : 3.8	1800	3.5	50 –150	120	15	1.94 – 1.98	0.0052
Second SiN <sub>x</sub> layer	NH <sub>3</sub> : 250			250	480	70	2.03	0.0012

<sup>a</sup>*FR* is flow rate of source gases

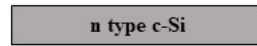
<sup>b</sup>*T*<sub>cat</sub> is temperature of catalyzer wire

<sup>c</sup>*P*<sub>g</sub> is gas pressure

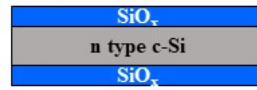
Table II. Thickness (nm) and *n* of SiO<sub>x</sub> layer formed by annealing at 350 °C for 30 min under various ambient conditions.

	Thickness	<i>n</i>
O <sub>2</sub> ambient	1.3	1.3
N <sub>2</sub> ambient	0.8 ~ 1	1.35

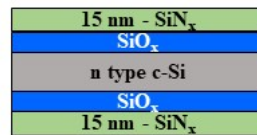
(1) Removing native  $\text{SiO}_x$  layers by 5% HF solution.



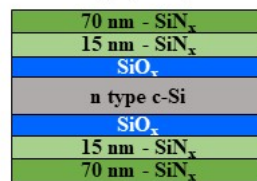
(2) Forming  $\text{SiO}_x$  layers by annealing at 350 °C for 30 min in  $\text{O}_2$  or  $\text{N}_2$ .



(3) Depositing the first  $\text{SiN}_x$  layers by Cat-CVD at  $T_{sub} < 150$  °C.



(4) Depositing the second  $\text{SiN}_x$  layers by Cat-CVD at  $T_{sub} = 250$  °C.



(5) Post-deposition annealing at 350 °C – 30 min in air ambient

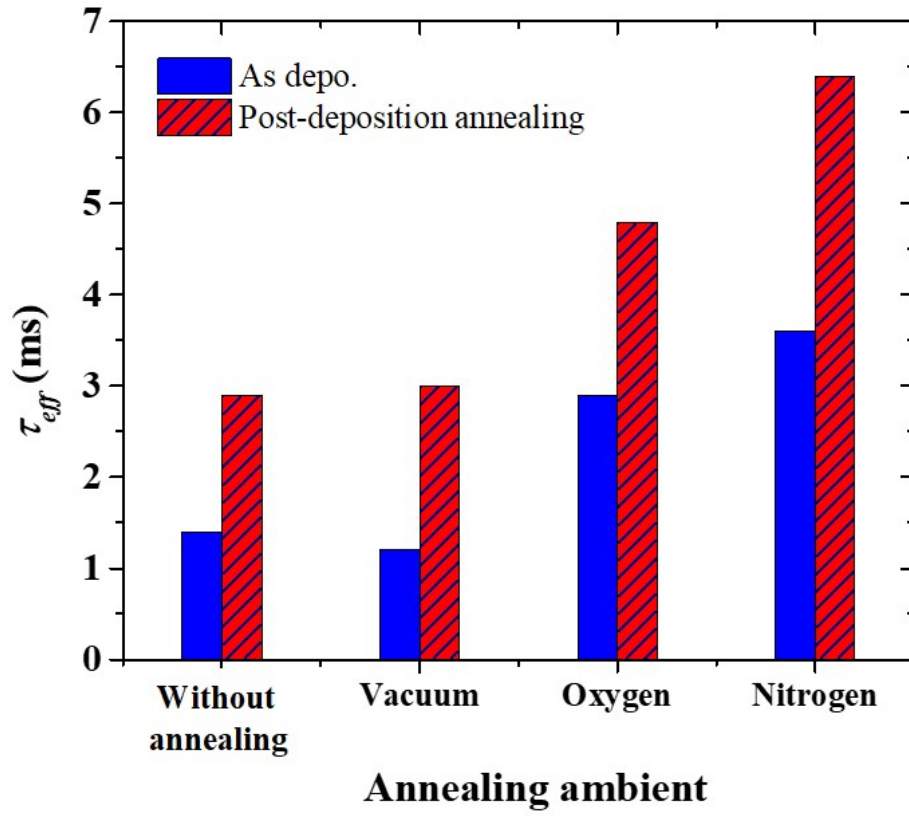


Fig. 2

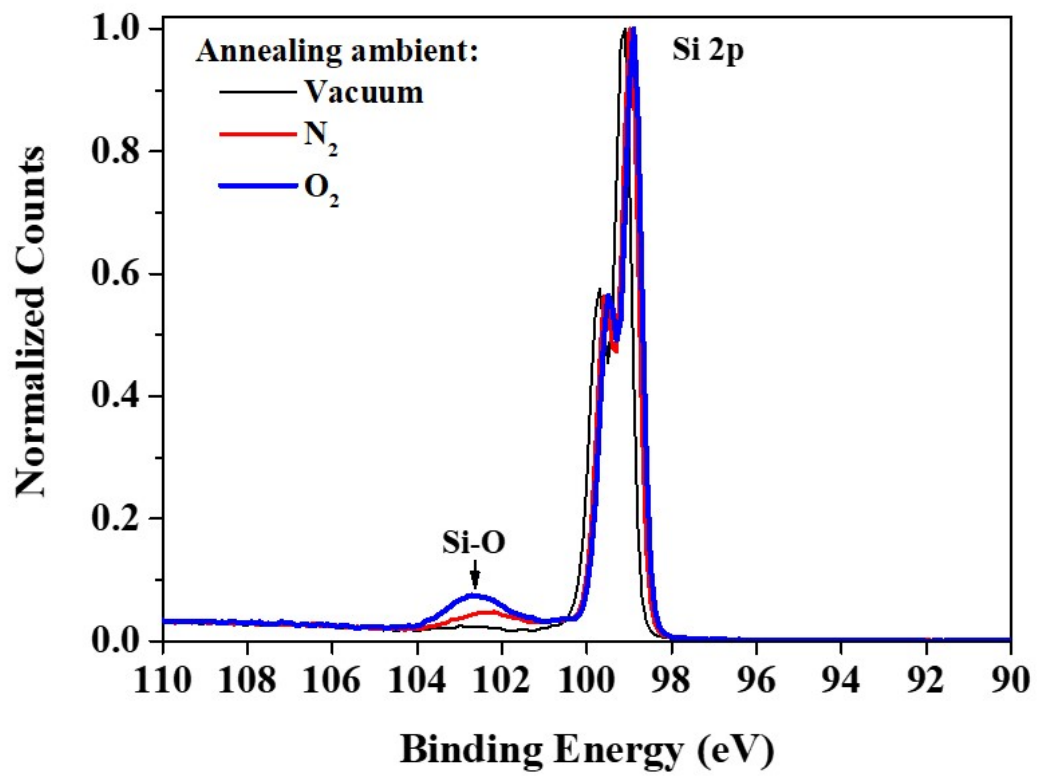


Fig. 3



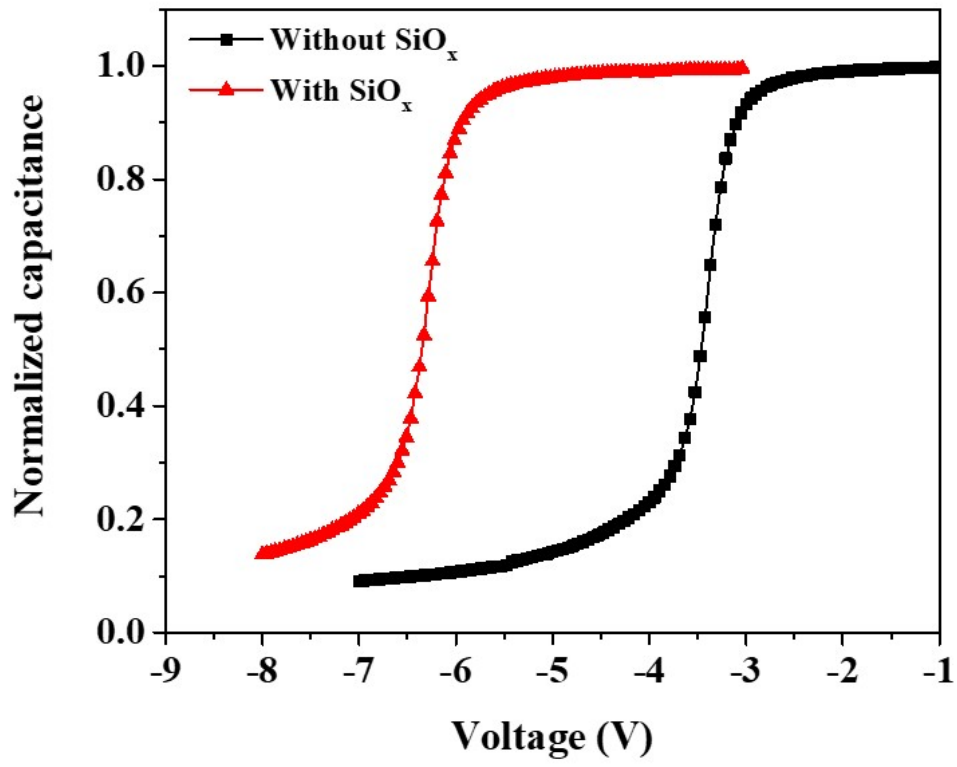


Fig. 4

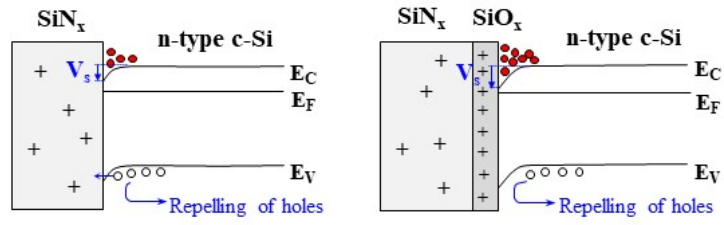


Fig. 5

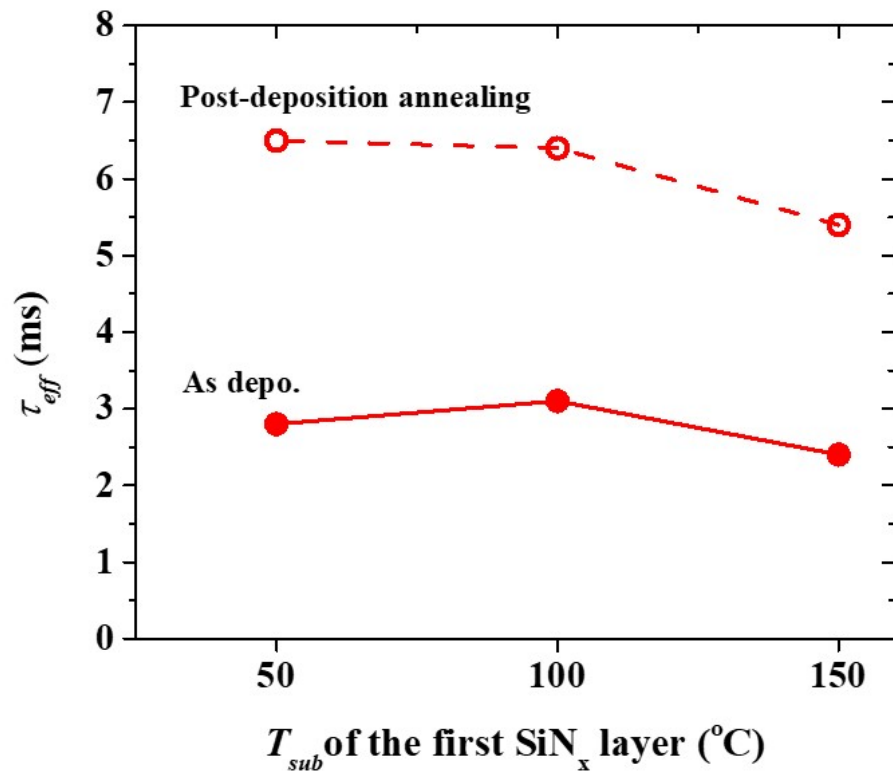


Fig. 6

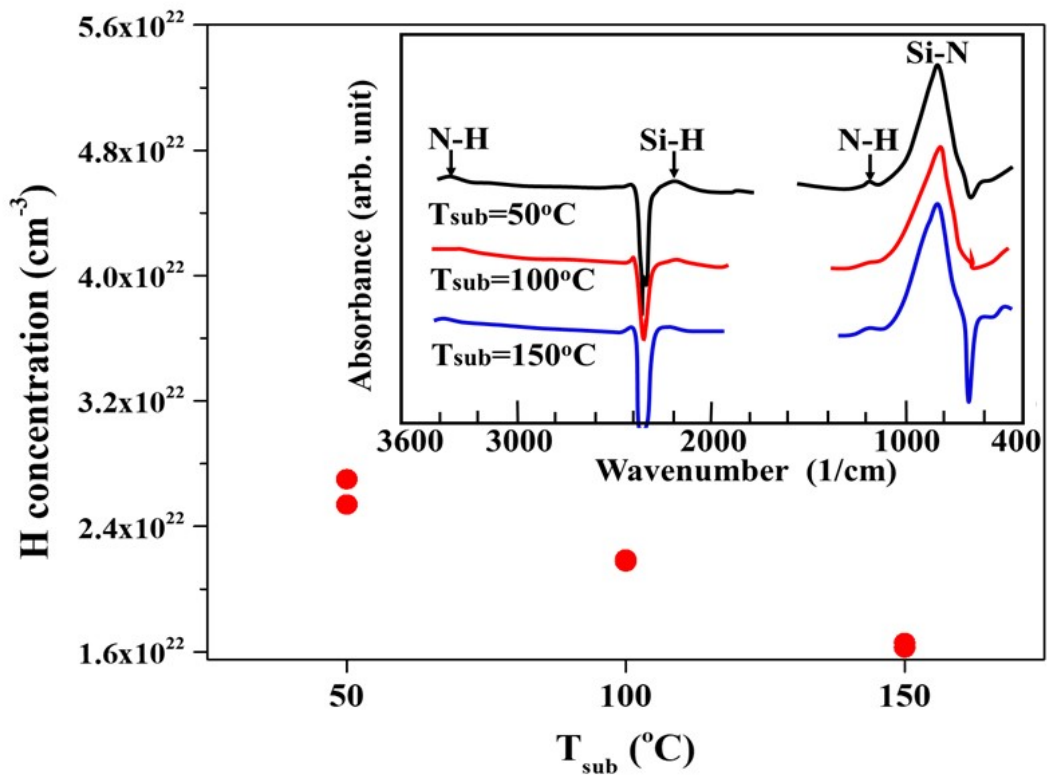


Fig. 7

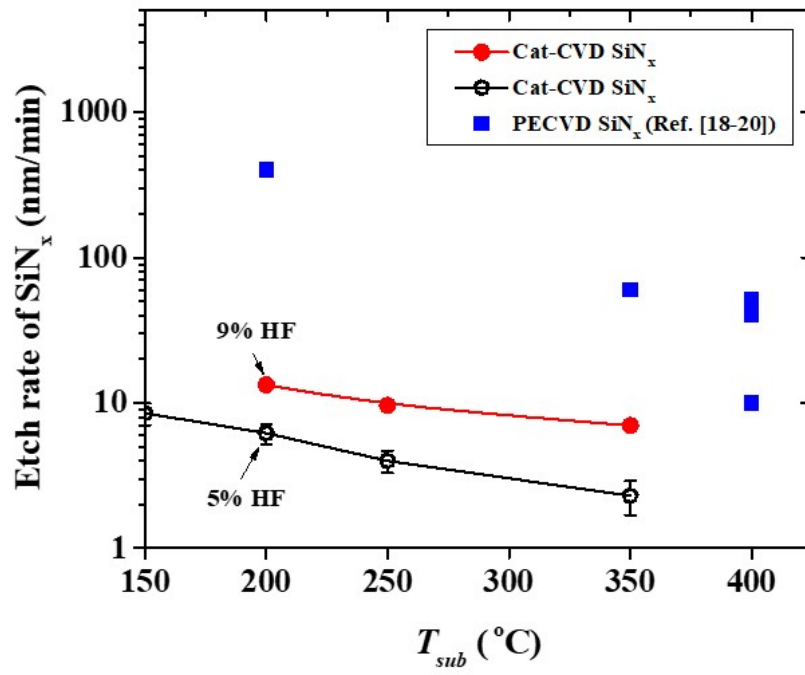


Fig. 8